

## EFFECT OF PERPENDICULAR A.C. ELECTRIC FIELD ON THE OBLIQUE WHISTLER MODE INSTABILITY IN THE EARTH'S MAGNETOSPHERE

A. K. TRIPATHI and R. P. SINGHAL

*Department of Applied Physics, Institute of Technology, Banaras Hindu University, Varanasi,  
221 005, India*

*(E-mail: aktrip2001@yahoo.co.in, rpsinghal@bhu.ac.in)*

(Received 11 September 2004; Accepted 26 September 2005)

**Abstract.** The elements of dielectric tensor and dispersion relation for obliquely propagating whistler waves with finite  $k_{\perp}$  in an infinite magnetoplasma are obtained for a kappa distribution in the presence of perpendicular a.c. electric field. Integrals and modified plasma dispersion functions are reduced in power series form. Numerical calculations have been performed to obtain temporal growth rate and real frequencies of the plasma waves for magnetospheric plasma, using linear theory of dispersion relation. The effect and modification introduced by the perpendicular a.c. electric field on the temporal growth rates, real frequencies and resonance condition are discussed for kappa and Maxwellian distributions. Our results and their interpretation are compared with known whistler observations obtained by ground-based techniques and satellite observations.

**Keywords:** A.c. electric field, instability, magnetosphere, whistler

### 1. Introduction

A theory for the generation of oblique electromagnetic waves from resonance with energetic charged particle was developed several years ago (Kennel and Wong, 1967). Most of the previous theoretical works on wave-particle interaction instability have assumed a Maxwellian distribution for the background plasma in the magnetosphere. However, most of the natural space plasmas are observed to possess a non-Maxwellian high-energy tail. An appropriate particle distribution function, for modeling such plasmas, is the generalized Lorentzian (kappa) distribution, which is also known as kappa distribution function. In this distribution function, characterization is done by spectral index  $\kappa$ , which for various values of  $\kappa$  assumes different shapes (Summers and Thorne, 1991). At high velocities, distribution  $\propto$  particle energy <sup>$-(\kappa + 1)$</sup> , i.e. the distribution has an inverse power-law tail in energy with exponent  $\kappa + 1$ . An important property of the kappa distribution is that in the limit as  $\kappa \rightarrow \infty$  it approaches to Maxwellian distribution function. Kappa distribution functions have also been used earlier to analyze and interpret spacecraft data in different regions of the Earth's magnetospheric plasma,

solar wind and planetary magnetospheres (Vasyliunas, 1968; Abraham-Shrauner et al., 1979; Leubner, 1982, Armstrong et al., 1983; Mace, 1998). On purely theoretical grounds in both space and laboratory plasmas, Hasegawa et al. (1985) showed that a plasma in the presence of superthermal particles suffers velocity-space diffusion. This enhanced diffusion produces a power law distribution at velocity much larger than the electron thermal speed. Stability analysis for the most space plasmas should therefore be performed using a kappa distribution rather than a Maxwellian. The presence of high-energy tail component in a kappa distribution considerably changes the rate of resonant energy transfer between particles and plasma waves, so that the conditions for the instability may be different for the two distributions.

Artificially triggered emissions in the magnetosphere have also been studied by various workers by signals transmitted from ground stations (Helliwell et al., 1973; Kimura, 1968 and references cited therein). There have been active VLF injection experiments also reported in the magnetosphere by ISEE-A spacecraft (Bell and Helliwell, 1978) including the Explorer 45 and IMP 6 observations. Injected electrical pulse and continuous wave from a VLF transmitter have also been reported to generate VLF and ULF waves in the magnetosphere (Inan et al., 1977). Space-time evolution of whistler mode wave growth in the magnetosphere triggered by injection of single a.c. frequency (2–6 kHz) signals was studied by Carlson et al. (1990). In all these experiments minimum initial amplitude of a.c. signal is required to trigger the whistler emissions. Once the triggering has started, further increase of magnitudes does not affect or enhance the triggering mechanism except the frequency of a.c. signals (Misra and Pandey, 1995 and the references cited therein). The behavior of high frequency a.c. electric field has also been studied to excite or quench the instabilities in the plasma (Prasad, 1967). In addition, electric fields have been measured at magnetospheric heights along and perpendicular to the Earth's magnetic field by various satellites such as ISEE, GEOS, S3, CRRES, DMSP and Viking (Mozer et al., 1978; Fälthammar, 1989; Lindqvist and Marklund, 1990; Burke and Maynard 2000). Fälthammar (1989) has reported measurements of fluctuating perpendicular electric fields  $\leq 10$  mV/m in the magnetosphere. Perpendicular electric fields of similar magnitude have been measured in the inner magnetosphere (Burke and Maynard, 2000). High-altitude perpendicular electric fields in the range 5–10 mV/m have also been measured by Viking Satellite (Lindqvist and Marklund, 1990).

The purpose of this study is to examine the influence of perpendicular a.c. electric field on the instability of obliquely propagating whistler waves due to kappa distribution. Further, it would be important to see how the whistler emissions are affected in the presence of a.c. electric field in the Earth's magnetosphere. Recently, the generation of parallel whistler mode instability in a variety of physical situations in the presence of perpendicular a.c. field

for kappa distribution was made (Tripathi and Misra, 2001, 2002) by method of characteristics using kinetic approach. In this paper, the study is further generalized for obliquely propagating whistler wave. This study would be useful in simulation experiments using the details of particle trajectories affected by a.c. electric field with a close look into the microscopic picture of wave-particle interactions. This would also be of relevance to triggered emissions and active satellite experiment leading to triggered emissions. The injected wave signals observed on satellites have shown spectral broadening and side bands (Bell et al., 1983; Tanaka et al., 1987). These have been explained by both linear (Bell and Ngo, 1990) and nonlinear wave-wave interactions (Chian et al. 1994). The nonlinear amplification (or damping) of whistler and electrostatic waves propagating in nonuniform media has been studied by Asseo et al. (1972) for electrostatic waves. The same results have been restated in whistler wave language by Roux (1974). Budko et al. (1971, 1972) have done the theoretical study of nonlinear effects related to whistler mode instabilities in magnetosphere assuming the waves to be monochromatic. These authors have considered the evolution of the distribution function for resonant electrons and obtained the expression for instability growth rate for nonlinear case. Vomvouridis et al. (1982) have also examined a nonlinear interaction process caused by electron trapping in a whistler wave propagating along a nonuniform magnetic field. The nonlinear effects are, however, not considered in this work.

In the present paper in Section 2, the elements of dielectric tensor for a kappa distribution in the presence of perpendicular a.c. electric field using kinetic approach and method of characteristics are obtained. The resulting modified dispersion relation by perpendicular a.c. electric field for oblique whistler waves is obtained using modified plasma dispersion function (Summers and Thorne, 1991). Further, growth rate and real frequency are directly obtained by numerical analysis using series solutions of general dispersion relation without having any further approximations than  $\lambda \rightarrow 0$  and  $k_{\perp} \ll k_{\parallel}$ . This generalized series dispersion relation may be reduced for Maxwellian distribution also by letting  $\kappa \rightarrow \infty$  for the same plasma parameters. Numerical results for the wave growth rate can be obtained when the phase velocity is much larger than electron thermal velocity. These numerical solutions are compared with respective solutions obtained for a Maxwellian distribution. The results and discussion for both types of distribution functions are given in Section 3. The conclusions are given in Section 4.

## 2. Dielectric Tensor and Dispersion Relation

We assume that zero-order quantities i.e., the density and composition of the plasma and the background magnetic field are static in time and uniform in

space. The plasma under consideration is of infinite extent, spatially homogeneous, anisotropic, embedded with a uniform magnetic field  $\mathbf{B}_0 (= B_0 \hat{e}_z)$  and an electric field  $E_0 \sin vt \hat{e}_x$ . In order to obtain general dielectric tensor and dispersion relation for linear theory of oblique propagation, the Vlasov–Maxwell equations are linearized. The small perturbations in electric and magnetic wave fields and distribution function  $\mathbf{E}_1$ ,  $\mathbf{B}_1$ , and  $f_1$  are assumed to have harmonic dependence of the form  $e^{i(\mathbf{k}\cdot\mathbf{r}-\omega t)}$ . The unperturbed and perturbed particle trajectories and velocities in the presence of perpendicular a.c. field have been obtained by solving zero and first order equation of motion using the geometry given in Figure 1 and following (i.e., Stix, 1962; Misra and Pandey, 1995; Tripathi and Misra, 2002).

For the ambient plasma, the particle distribution function is assumed to be anisotropic kappa distribution function and is given as :

$$f_{s_0}^\kappa(\mathbf{v}) = \frac{1}{\pi^{3/2} \theta_{\perp s}^2 \theta_{\parallel s} \kappa^{3/2}} \frac{\Gamma(\kappa + 1)}{\Gamma(\kappa - \frac{1}{2})} \left[ 1 + \frac{\mathbf{v}_{\parallel}^2}{\kappa \theta_{\parallel s}^2} + \frac{\mathbf{v}_{\perp}^2}{\kappa \theta_{\perp s}^2} \right]^{-(\kappa+1)} \quad (1)$$

with associated effective thermal speeds and temperatures parallel and perpendicular to the ambient magnetic field as :

$$\theta_{\parallel s} = [(2\kappa - 3)/\kappa]^{1/2} (T_{\parallel s}/m_s)^{1/2}, \quad \theta_{\perp s} = [(2\kappa - 3)/\kappa]^{1/2} (T_{\perp s}/m_s)^{1/2} \quad (2)$$

and the temperature anisotropy  $A_{T_s}^\kappa$  defined by

$$A_{T_s}^\kappa = \frac{T_{\perp s}}{T_{\parallel s}} - 1 = \frac{\theta_{\perp s}^2}{\theta_{\parallel s}^2} - 1 \quad (3)$$

where,  $\kappa$  is the spectral index of the distribution (The parameter  $\kappa$  generally takes on positive integral values  $> 2$ ) and  $\Gamma$  is the gamma function. By using

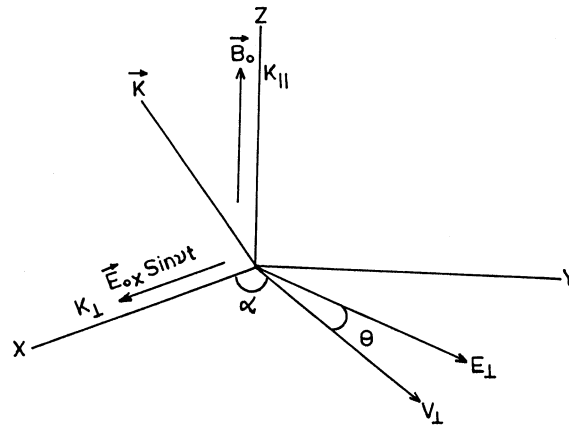


Figure 1. Geometry of the problem.

dielectric tensor, the dispersion relation is obtained from the condition for nontrivial solutions of (Stix, 1962; Sazhin, 1993; Summers et al., 1994).

$$D = A^* N^4 + B^* N^2 + C^* = 0 \quad (4)$$

where

$$\begin{aligned} A^* &= \epsilon_{11} \sin^2 \psi + 2 \epsilon_{13} \sin \psi \cos \psi + \epsilon_{33} \cos^2 \psi \\ B^* &= -\epsilon_{11} \epsilon_{33} - (\epsilon_{22} \epsilon_{33} + \epsilon_{23}^2) \cos^2 \psi - (\epsilon_{11} \epsilon_{22} + \epsilon_{12}^2) \sin^2 \psi \\ &\quad + 2(\epsilon_{12} \epsilon_{23} - \epsilon_{22} \epsilon_{13}) \sin \psi \cos \psi + \epsilon_{13}^2 \\ C^* &= \epsilon_{33} (\epsilon_{11} \epsilon_{22} + \epsilon_{12}^2) + \epsilon_{11} \epsilon_{23}^2 + 2 \epsilon_{12} \epsilon_{13} \epsilon_{23} - \epsilon_{22} \epsilon_{13}^2 \end{aligned}$$

Here  $N = ck/\omega$ ,  $\psi$  is the angle between  $\mathbf{k}$  and  $\mathbf{B}_0$ . Equation (4) is known convenient form of general dispersion relation for the linear theory of oblique waves in a hot magnetized plasma and the different instabilities may be studied by simplifying this equation. The components of dielectric tensor  $\epsilon_{ij}$  in the presence of perpendicular a.c. electric field are given in the Appendix A.

The linear theory of whistler-mode propagation is based on the assumption that waves with different frequencies and wave numbers do not interact with each other and that the waves do not cause any systematic change in the background particle distribution function  $f_0$ . When plasma instabilities are excited and waves grow, a number of nonlinear phenomena appear which modify the plasma states. Nonlinear effects become important when the wave energy density becomes much larger than at the thermal equilibrium. The ratio of the wave energy density and the thermal energy density,  $(W/n_0 T)$ , is used as a measure of turbulence. At an early stage of development the system has a response that obeys the linear dispersion relation and as the amplitude grows larger the nonlinearity modifies the linear properties. The particle motions in the plasma are effected by the waves. The wave spectrum spreads out because of the nonlinear wave-wave interactions as well as the nonlinear wave-particle interactions (Hasegawa, 1975; Inan et al., 1978; Vomvoridis et al., 1982; Sazhin, 1993). The nonlinear effects are, however, not included in the present work.

### 3. Results and Discussion

A numerical procedure without any further approximations is followed for solving the general dispersion relation given in Equation (4). The kappa distribution given in (1) has been used in case of obliquely propagating electron whistler mode waves in the presence of perpendicular a.c. electric field in the Earth's magnetosphere. The contribution of specific positive integral values of spectral index  $\kappa$  i.e.,  $\kappa > 2$ , amplitude and frequency of a.c.

signal are included. The change in the values of  $\kappa$  gives the different models of distribution functions for space plasmas, e.g. plasmas in planetary magnetosphere and the solar wind, as well as astrophysical plasmas. The normalized temporal growth rate have been studied for various specific values of spectral index  $\kappa$ , amplitude and frequency of a.c. signal and for various wave normal angles ( $\psi$ ) of propagation in case of representative magnetospheric plasma at geostationary height of  $L=6.6$  with  $\mathbf{B}_0=10^{-7}$  Tesla along with other plasma parameters.

The values of a.c. electric field have been taken  $E_0 \leq 10$  mV/m. The university of Iowa plasma wave experiment on Explorer 45 and IMP 6 (Inan et al., 1977; Misra and Pandey, 1995) have shown the feasibility of wave injection experiment from orbiting satellites having sine wave signals of (1–10 kHz) and accordingly, a.c. frequencies in this range have been used in calculations. The particle populations have a kappa distribution with  $\kappa$  lying in the range of  $2 \leq \kappa \leq 6$  (Summers and Thorne, 1991; Xue et al., 1996; Mace, 1998) with a reasonable temperature anisotropy  $A_{T_s}^{\kappa} = 0.25-1.0$  consistent with the observations obtained in Earth's magnetosphere. The particle density  $N_0 = (1-3) \times 10^6 \text{ m}^{-3}$ , is assumed. In a temporal growth rate a real value of wave vector  $\mathbf{k}$  is prescribed in Equation (4). Initially a value of the complex wave frequency  $\omega$  is assumed. Then it is solved numerically by iteration on  $\omega$ . Hence a complex root  $\omega = \omega_R + i\omega_\ell$  is found in which  $\omega_\ell > 0$ , leads to damping and  $\omega_\ell < 0$  leads to growth.

Figure 2 shows the variation of normalized temporal growth rate  $\gamma$  with normalized wave number  $\bar{\mathbf{K}}$  for oblique electron whistler mode instability for various values of a.c. field frequency. Other fixed values of plasma parameter are seen in figure caption. We first consider the sensitivity of a.c. frequency on the different values of  $\kappa$ , which is a measure of the relative number of particles in high-energy tail of the distribution (Xue et al., 1996). The choice of particle distribution function modifies the dielectric tensor, plasma dispersion function and ultimately the solution of whistler mode dispersion relation. Thus a change in  $\kappa$  and frequency of a.c. signal affect the growth rate. This aspect is demonstrated in following graphs. A direct comparison is made between the results for the kappa ( $\kappa=3$ ) and Maxwellian distributions ( $\kappa=\infty$ ). The temporal growth rate of wave increases as the a.c. frequencies increases (2–8 kHz). In case of Maxwellian distribution, the temporal growth are larger in comparison to that of kappa distribution. The a.c. frequency increases the growth rate in comparison to the growth rate without a.c. frequency ( $\nu=0$ ). A.C. frequency affects the temporal growth rate while its magnitude has a marginal effect. This phenomena is similar to triggered whistler emissions, where a minimum initial magnitude of a.c. frequency is required to trigger the instability and once the instability starts it has no further role. This result is also in agreement with the observations of triggering emissions seen by Kimura (1968) and simulation studies of Molvig

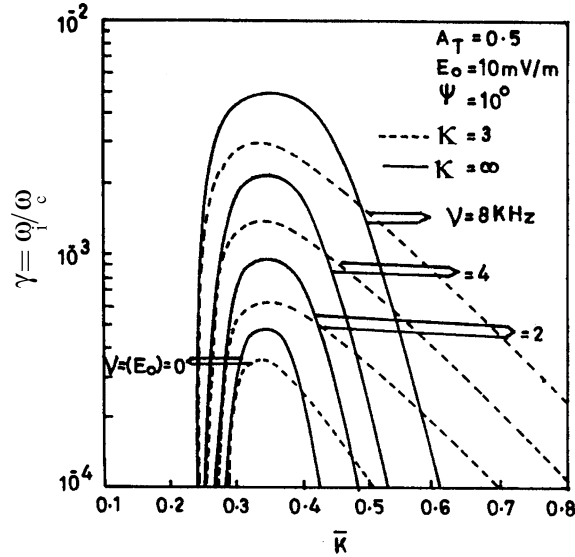


Figure 2. Dependence of the normalized temporal growth rate  $\gamma = (\omega_r/\omega_c)$  on the normalized wave number  $\bar{K} = (k_{\parallel}\theta_{\parallel}/\omega_c)$  of the oblique electron whistler instability for various values of the a.c. field frequencies  $\nu$ .

et al. (1988). The shift of maxima to lower  $\bar{K}$  as a.c. frequency increases shows that emission frequencies are shifted to lower values of frequency. The maximum growth rate and corresponding  $\bar{K}$  gives the emitted frequency in the range of (1–2 kHz) as observed at ground station (Lalmani et al., 2000) and satellite (Helliwell, 1965).

Effect of a.c. frequencies on the normalized temporal growth rate versus normalized real frequency  $X$  of the oblique electron whistler mode instability with fixed plasma parameters are shown in Figure 3. This figure provides directly the emitted frequencies of both distributions. The emission frequency ( $f = \omega_r/2\pi$ ) are found in the range of (1.14–1.29 kHz) corresponding to the change of values of a.c. frequencies (2–8 kHz) in agreement with observations by Carlson et al. (1990). The temporal growth rate and emitted frequencies are little higher for Maxwellian than kappa distribution. Normally, observed values of  $\kappa$  lies in the range of  $2 \leq \kappa \leq 6$ . Therefore, it is concluded that Maxwellian distribution overestimates peak wave growth. This fact is very similar to calculations (Xue et al., 1996). Emitted frequencies are in agreement with low latitude ground-based observations (Lalmani et al., 2000). The temperature anisotropy for electron in such case is 0.5 which is dominant source to generate the instability at equatorial magnetospheric height in both distributions.

Effect of propagation angles on normalized temporal growth rate are shown in Figure 4. The temporal growth rate is more at small angles showing

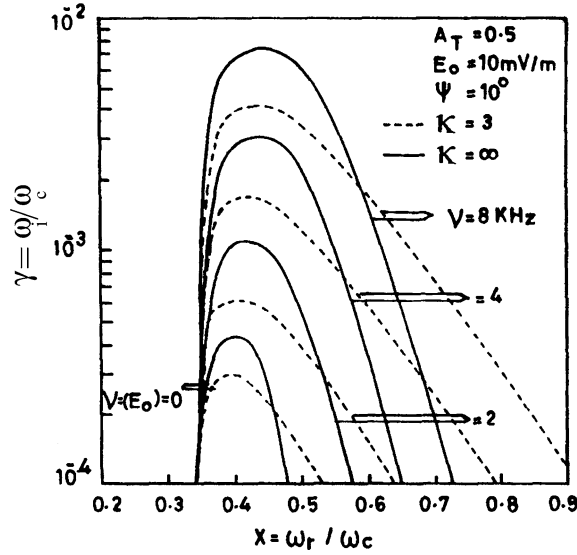


Figure 3. Dependence of the normalized temporal growth rate  $\gamma$  on the normalized real frequency  $X = \omega_r / \omega_c$  of the oblique electron whistler instability for various values of a.c. field frequencies  $\nu$ .

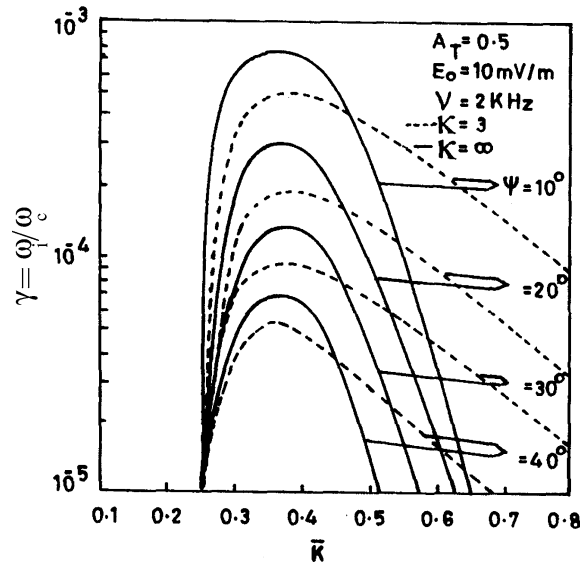


Figure 4. Dependence of the normalized temporal growth rate on the normalized wave number of the oblique electron whistler instability for various values of the wave normal angles  $\psi$  of propagation.

the possibility of whistler generation within a narrow cone of angles with magnetic field (Sazhin, 1993). This effect can be seen more clearly in Figure (5) where variation of normalized growth rate with normalized real



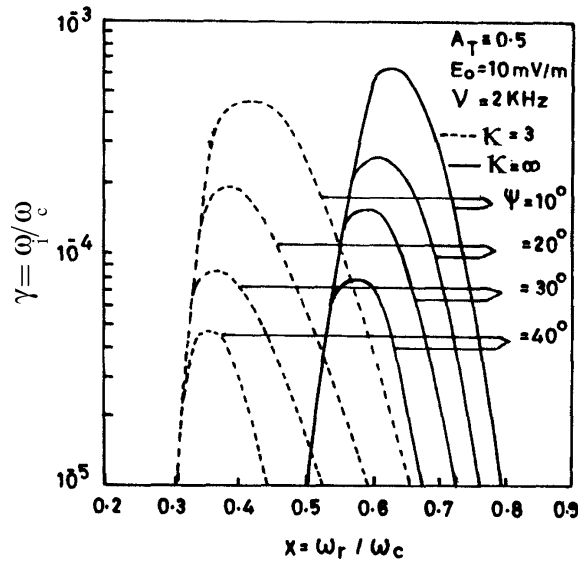


Figure 5. Dependence of the normalized temporal growth rate on the normalized real frequency of the oblique electron whistler instability for various wave normal angles of propagation.

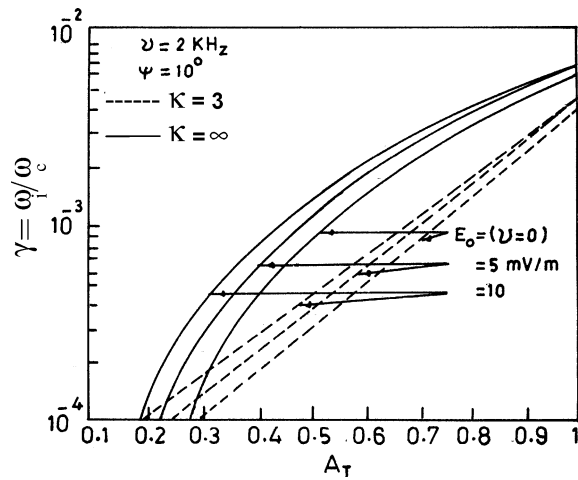


Figure 6. Dependence of normalized temporal growth rate on temperature anisotropy  $A_{T_s}^k$  of the oblique electron whistler instability for various values of the amplitude of a.c. field  $E_0$ .

frequency are shown. Whistler mode growth rate reduces fast as the angle increases beyond  $30^\circ$ . Similar observations were reported by Zhang et al. (1993) where they have shown minor change in the peak growth rate when  $\psi$

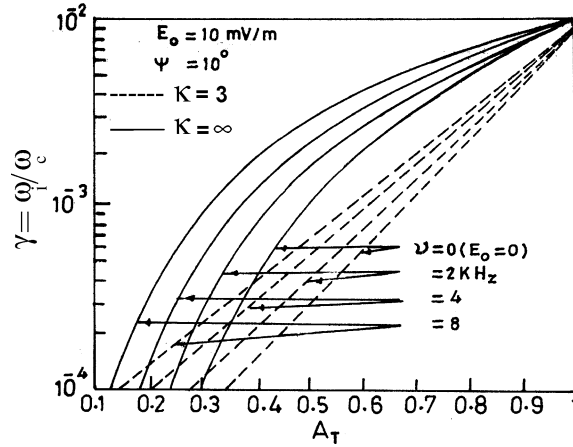


Figure 7. Dependence of normalized temporal growth rate on temperature anisotropy of the oblique electron whistler instability for various values of the a.c. field frequencies.

increases ( $0^\circ$ – $30^\circ$ ). The growth rate starts to decrease rapidly with  $\psi > 30^\circ$ , and reaches 0 when  $\psi$  is near  $80^\circ$ .

Figures 6 and 7 show the effect of amplitude and a.c. frequency variation on temporal growth rate for different values of temperature anisotropy  $A_{T_s}^\kappa$ . The growth rate increases with temperature anisotropy when both amplitude changes (5–10 mV/m) and a.c. frequency changes (2–8 kHz) in both cases, except that maximum growth rate is higher in the case of Maxwellian distribution. Further, it shows that Maxwellian distribution is more sensitive to temperature anisotropy than the kappa distribution. It is also seen from these figures that the effect of both amplitude and frequency of the a.c. field decreases when  $A_{T_s}^\kappa$  goes to higher values and that the choice of the amplitude and a.c. frequency affects the growth rate substantially.

#### 4. Conclusion

Oblique whistler waves are significantly affected by the presence of perpendicular a.c. electric field. Especially, its frequency affects the growth rate. The growth rates for electron whistler are more in general for Maxwellian than for kappa distribution even at small angles of propagation ( $\psi \leq 10^\circ$ ). In case of Maxwellian distribution, emitted frequencies are little higher than those obtained for kappa distribution at arbitrary wave normal angle. In case of kappa distribution, the emitted frequencies are quite different and widely separated as the angle of propagation increases, whereas in case of Maxwellian distribution their separations are far less. Thus the parallel propagating whistler shall give different wave gain and frequency of emissions

compared to those obtained from oblique propagating whistlers. However, gain decreases as the angle increases. Thus the presence of temperature anisotropy is the prominent source of providing free energy and of generating whistler mode instability in both plasma, whereas the a.c. field is acting as the triggering mechanism to excite the instability within the magnetosphere. Such results could explain the low frequency whistler emissions observed at ground and magnetospheric heights.

### Acknowledgements

The authors gratefully acknowledge the computational help by Shri Girish Chandra of I.E.T., Lucknow, India. This work was supported by a Research Associateship awarded to one of the author (A.K.T.) by the Council of Scientific and Industrial Research, Government of India.

### 5. Appendix A

Components of dielectric tensor  $\epsilon_{ij}$

$$\begin{bmatrix} \epsilon_{11}-1 \\ \epsilon_{12} \\ \epsilon_{22}-1 \end{bmatrix} = \sum_s \frac{\omega_{ps}^2}{\omega^2} \frac{1}{\lambda^2} \sum_{n=-\infty}^{+\infty} \begin{bmatrix} n^2 \\ \text{in} \\ -1 \end{bmatrix} \times \left\{ A_{T_s}^\kappa \begin{bmatrix} S_1 \\ S_3 \\ S_5 \end{bmatrix} + \left( A_{T_s}^\kappa \xi + \frac{\omega}{k_{\parallel} \theta_{\parallel s}} \right) \begin{bmatrix} S_2 \\ S_4 \\ S_6 \end{bmatrix} \right\} \quad (\text{A1})$$

$$\begin{bmatrix} \epsilon_{13} \\ \epsilon_{23} \\ \epsilon_{33}-1 \end{bmatrix} = \sum_s \frac{\omega_{ps}^2 \theta_{\parallel s}}{\omega^2 \theta_{\perp s}} \sum_{n=-\infty}^{+\infty} \left( A_{T_s}^\kappa \xi + \frac{\omega}{k_{\parallel} \theta_{\parallel s}} \right) \times \begin{bmatrix} \sqrt{2}n/\lambda^{3/2} \\ -\sqrt{2}i/\lambda^{3/2} \\ 2\left(\frac{\theta_{\parallel s}}{\theta_{\perp s}}\right)\left(\frac{\xi}{\lambda}\right) \end{bmatrix} \left\{ \begin{bmatrix} S_1 \\ S_3 \\ S_1 \end{bmatrix} + \xi \begin{bmatrix} S_2 \\ S_4 \\ S_2 \end{bmatrix} \right\} \quad (\text{A2})$$

$$\text{with } \epsilon_{21} = -\epsilon_{12}, \quad \epsilon_{13} = \epsilon_{31}, \quad \epsilon_{32} = -\epsilon_{23} \quad (\text{A3})$$

where

$$S_1 = \frac{(\kappa - \frac{3}{2})(\kappa - \frac{5}{2})}{(\kappa - 2)^2} \int_0^\infty \frac{\lambda_1 J_n^2(\lambda_1) d\lambda_1}{(1 + \lambda_1^2/2\lambda(\kappa - 2))^{\kappa-1/2}} \quad (\text{A4})$$

$$\begin{aligned}
S_2 = & \left(\frac{\kappa-1}{\kappa-2}\right)^{3/2} \left(\frac{\kappa-\frac{5}{2}}{\kappa-2}\right) \left[ \int_0^\infty \frac{J_n^2(\lambda_1)}{(1+\lambda_1^2/2\lambda(\kappa-2))^\kappa} Z_{\kappa-1}^* \right. \\
& \times \left. \left\{ \lambda_1 \left( \frac{(\kappa-1)/\kappa-2}{(1+\lambda_1^2/2\lambda(\kappa-2))} \right)^{1/2} \xi \right\} d\lambda_1 \right. \\
& + \frac{v\epsilon_x}{(\omega_{c_s}^2 - v^2)} \left\{ \int_0^\infty \frac{J_p'(\lambda_2)}{(1+\lambda_1^2/2\lambda(\kappa-2))^\kappa} Z_{\kappa-1}^* \right. \\
& \times \left. \left. \left. \left( \frac{(\kappa-1)/\kappa-2}{(1+\lambda_1^2/2\lambda(\kappa-2))} \right)^{1/2} \xi \right\} d\lambda_2 \right] \tag{A5}
\end{aligned}$$

$$S_3 = \frac{(\kappa-\frac{3}{2})(\kappa-\frac{5}{2})}{(\kappa-2)^2} \int_0^\infty \frac{\lambda_1^2 J_n(\lambda_1) J_n'(\lambda_1) d\lambda_1}{(1+\lambda_1^2/2\lambda(\kappa-2))^{\kappa-\frac{1}{2}}} \tag{A6}$$

$$\begin{aligned}
S_4 = & \left(\frac{\kappa-1}{\kappa-2}\right)^{3/2} \left(\frac{\kappa-\frac{5}{2}}{\kappa-2}\right) \left[ \int_0^\infty \frac{\lambda_1 J_n(\lambda_1) J_n'(\lambda_1)}{(1+\lambda_1^2/2\lambda(\kappa-2))^\kappa} Z_{\kappa-1}^* \right. \\
& \times \left. \left\{ \lambda_1 \left( \frac{(\kappa-1)/(\kappa-2)}{(1+\lambda_1^2/2\lambda(\kappa-2))} \right)^{1/2} \xi \right\} d\lambda_1 \right. \\
& + \frac{v\epsilon_x}{(\omega_{c_s}^2 - v^2)} \left\{ \int_0^\infty \frac{J_p(\lambda_2)}{(1+\lambda_1^2/2\lambda(\kappa-2))^\kappa} Z_{\kappa-1}^* \right. \\
& \times \left. \left. \left. \left( \frac{(\kappa-1)/(\kappa-2)}{(1+\lambda_1^2/2\lambda(\kappa-2))} \right)^{1/2} \xi \right\} d\lambda_2 \right] \tag{A7}
\end{aligned}$$

$$S_5 = \frac{(\kappa-\frac{3}{2})(\kappa-\frac{5}{2})}{(\kappa-2)^2} \int_0^\infty \frac{\lambda_1^3 J_n^2(\lambda_1) d\lambda_1}{(1+\lambda_1^2/2\lambda(\kappa-2))^{\kappa-\frac{1}{2}}} \tag{A8}$$

$$\begin{aligned}
S_6 = & \left(\frac{\kappa-1}{\kappa-2}\right)^{3/2} \left(\frac{\kappa-\frac{5}{2}}{\kappa-2}\right) \left[ \int_0^\infty \frac{\lambda_1^2 J_n^2(\lambda_1)}{(1+\lambda_1^2/2\lambda(\kappa-2))^\kappa} Z_{\kappa-1}^* \right. \\
& \times \left. \left\{ \lambda_1 \left( \frac{(\kappa-1)/(\kappa-2)}{(1+\lambda_1^2/2\lambda(\kappa-2))} \right)^{1/2} \xi \right\} d\lambda_1 \right. \\
& + \frac{v\epsilon_x}{(\omega_{c_s}^2 - v^2)} \left\{ \int_0^\infty \frac{J'_p(\lambda_2) J_p(\lambda_2)}{(1+\lambda_1^2/2\lambda(\kappa-2))^\kappa} Z_{\kappa-1}^* \right. \\
& \times \left. \left. \left( \frac{(\kappa-1)/(\kappa-2)}{(1+\lambda_1^2/2\lambda(\kappa-2))} \right)^{1/2} \xi \right\} d\lambda_2 \right] \quad (A9)
\end{aligned}$$

with

$$\xi = \frac{\omega - n\omega_{c_s} + pv}{k_{\parallel} \theta_{\parallel s}}, \quad \lambda = \frac{1}{2} \left( \frac{k_{\perp} \theta_{\perp s}}{\omega_{c_s}} \right)^2 = (k_{\perp} \rho_{Ls})^{1/2} \quad (A10)$$

$$\begin{aligned}
J'_n &= \frac{dJ_n(\lambda_1)}{d\lambda_1}, \quad J'_p = \frac{dJ_p(\lambda_2)}{d\lambda_2} \\
\omega_{c_s} &= \frac{e_s \mathbf{B}_0}{m_s}, \quad \omega_{p_s}^2 = \frac{N_{0s} e_s^2}{\epsilon_0 m_s}, \quad \epsilon_x = \frac{e_s \mathbf{E}_{0x}}{m_s}
\end{aligned}$$

where  $J_n(\lambda_1)$  and  $J_p(\lambda_2)$  are the Bessel functions of first kind with the argument of  $\lambda_1$  and  $\lambda_2$  respectively and having the order  $n$  and  $p$ .  $J'_n(\lambda_1)$  and  $J'_p(\lambda_2)$  are the derivative with respect to  $\lambda_1$  and  $\lambda_2$ .  $\epsilon_0$ ,  $e_s$ ,  $m_s$  and  $N_{0s}$  are respectively permittivity of free space, particle charge, mass and number density of species  $s$ .  $\omega_{c_s}$  and  $\omega_{p_s}$  are gyrofrequency and plasma frequency, respectively.

The function  $Z_{\kappa-1}^*$  occurring in (A5), (A7) and (A9) is the modified plasma dispersion function (Summers and Thorne, 1991) which for integral values of  $\kappa \geq 2$  may be written as :

$$Z_{\kappa}^*(\xi) = -\frac{(\kappa - \frac{1}{2})}{2\kappa^{3/2}} \frac{\kappa!}{(2\kappa)!} \times \sum_{\ell=0}^{\kappa} \frac{(\kappa + \ell)!}{\ell!} i^{\kappa-\ell} \left( \frac{2}{(\xi/\sqrt{\kappa} + i)} \right)^{\kappa-\ell+1} \quad (A11)$$

In the presence of perpendicular a.c. electric field in the limit  $\lambda \rightarrow 0$  the integrals  $S_1, S_2, \dots, S_6$  are reduced to power series form (Summers et al., 1994).

$$S_1 = \frac{1}{2^{|n|}} \frac{\kappa^{|n|-1} \Gamma(\kappa - |n| + \frac{1}{2})}{\Gamma(|n| + 1) \Gamma(\kappa - \frac{1}{2})} \lambda^{(|n|+1)} + \dots \quad \text{if } \kappa > |n| - \frac{1}{2} \quad (\text{A12})$$

$$S_2 = \left( 1 + \frac{v\epsilon_x}{(\omega_{c_s}^2 - v^2)} \right) \frac{1}{2^{|n|}} \frac{\kappa^{|n|} \Gamma(\kappa - |n| - \frac{1}{2})}{\Gamma(|n| + 1) \Gamma(\kappa - \frac{1}{2})} \left( \frac{\kappa - |n|}{\kappa} \right)^{3/2} \\ \times \lambda^{(|n|+1)} Z_{\kappa-|n|}^* \left[ \left( \frac{\kappa - |n|}{\kappa} \right)^{1/2} \xi \right] + \dots \\ \text{if } \kappa \geq |n| + 1, \quad n \neq 0 \quad (\text{A13})$$

$$S_3 = \frac{1}{2^{|n|}} \frac{\kappa^{|n|-1} \Gamma(\kappa - |n| + \frac{1}{2})}{\Gamma(|n|) \Gamma(\kappa - \frac{1}{2})} \lambda^{(|n|+1)} + \dots \quad \text{if } \kappa > |n| - \frac{1}{2} \text{ and } n \neq 0, \quad (\text{A14})$$

$$S_4 = \left( 1 + \frac{v\epsilon_x}{(\omega_{c_s}^2 - v^2)} \right) \frac{1}{2^{|n|}} \frac{\kappa^{|n|} \Gamma(\kappa - |n| - \frac{1}{2})}{\Gamma(\kappa - \frac{1}{2}) \Gamma(|n|)} \left( \frac{\kappa - |n|}{\kappa} \right)^{3/2} \\ \times \lambda^{(|n|+1)} Z_{\kappa-|n|}^* \left[ \left( \frac{\kappa - |n|}{\kappa} \right)^{1/2} \xi \right] + \dots \\ \text{if } \kappa \geq |n| + 1, \text{ and } n \neq 0 \quad (\text{A15})$$

$$S_5 = \frac{|n|}{2^{|n|}} \frac{\kappa^{|n|-1} \Gamma(\kappa - |n| + \frac{1}{2})}{\Gamma(|n|) \Gamma(\kappa - \frac{1}{2})} \times \lambda^{(|n|+1)} + \dots \quad \text{if } \kappa > |n| - \frac{1}{2} \text{ and } n \neq 0, \quad (\text{A16})$$

$$S_6 = \left( 1 + \frac{v\epsilon_x}{(\omega_{c_s}^2 - v^2)} \right) \frac{|n|}{2^{|n|}} \frac{\kappa^{|n|} \Gamma(\kappa - |n| - \frac{1}{2})}{\Gamma(\kappa - \frac{1}{2}) \Gamma(|n|)} \left( \frac{\kappa - |n|}{\kappa} \right)^{3/2} \\ \times \lambda^{(|n|+1)} Z_{\kappa-|n|}^* \left[ \left( \frac{\kappa - |n|}{\kappa} \right)^{1/2} \xi \right] + \dots \\ \text{if } \kappa \geq |n| + 1, \text{ and } n \neq 0 \quad (\text{A17})$$

## References

- Abraham-Shrauner, B., Asbridge, J. R., Bame, S. J., and Feldman, W. C.: 1979, *J. Geophys. Res.* **84**, 553.
- Armstrong, T. P., Paonessa, M. T., Bell, E. V. II, and Krimigis, S. M.: 1983, *J. Geophys. Res.* **88**, 8893.
- Asseo, E., Laval, G., Pellat, R., Welti, R., and Roux, A.: 1972, *J. Plasma Phys.* **8**, 341.
- Bell, T.F. and Helliwell, R. A.: 1978, *ISEE Trans. Geosci. Elect.* GE-16.
- Bell, T. F., James, H. G., Inan, U. S., and Katsufakis, J. P.: 1983, *J. Geophys. Res.* **88**, 4813–4840.
- Bell, T. F. and Ngo, H. D.: 1990, *J. Geophys. Res.* **95**, 149–172.
- Budko, N. I., Karpman, V. I., and Pokhotelov, O. A.: 1971, *JETP. Lett.* **14**, 112.
- Budko, N. I., Karpman, V. I., and Pokhotelov, O. A.: 1972, *Cosmic Electrodyn.* **3**, 147.
- Burke, W. J. and Maynard, N. C.: 2000, *IEEE Trans. Plasma Sci.* **28**, 1903.
- Carlson, C. R., Helliwell, R. A., and Inan, U. S.: 1990, *J. Geophys. Res.* **95**, 15073.
- Chian, A. C.-L., Lopes, S. R., and Alves, M. V.: 1994, *Astron. Astrophys.* **288**, 981–984.
- Fälthammar, C. G.: 1989, *IEEE Trans. Plasma Sci.* **17**, 174.
- Hasegawa, A.: 1975, *Plasma Instabilities and Nonlinear Effects*, Springer-Verlag, Berlin.
- Hasegawa, A., Mima, K., and Duong-Van, M.: 1985, *Phys. Rev. Lett.* **54**, 2608.
- Helliwell, R. A.: 1965, *Whistler and Related Ionospheric Phenomena*, Stanford University Press, Stanford, California, 288–308 pp.
- Helliwell, R. A., Katsufakis, J. P., and Trimpf, M. L.: 1973, *J. Geophys. Res.* **78**, 4679.
- Inan, U. S., Bell, T. F., and Carpenter, D. L.: 1977, *J. Geophys. Res.* **82**, 1177.
- Inan, U. S., Bell, T. F., and Helliwell, R. A.: 1978, *J. Geophys. Res.* **83**, 3235–3253.
- Kennel, C. F. and Wong, H. V.: 1967, *J. Plasma Phys.* **1**, 81.
- Kimura, I.: 1968, *J. Geophys. Res.* **73**, 4451.
- Lalmami, M. K. B., Kumar, R., Singh, R., and Gwal, A. K.: 2000, *Indian J. Phys.* **74B**, 117.
- Leubner, M. P.: 1982, *J. Geophys. Res.* **87**, 6335.
- Lindqvist, P. A. and Marklund, G. T.: 1990, *J. Geophys. Res.* **95**, 5867.
- Mace, R. L.: 1998, *J. Geophys. Res.* **103**, 14643.
- Misra, K. D. and Pandey, R. S.: 1995, *J. Geophys. Res.* **100**, 19405.
- Molvig, K., Hilfer, G., Miller, R. H., and Myczkowski, J.: 1988, *J. Geophys. Res.* **93**, 5665.
- Mozer, F. S., Torbert, R. B., Fahleson, U. V., Fälthammar, C. G., Gonafalone, A., Pedersen, A., and Russel, C. T.: 1978, *Space. Sci. Rev.* **22**, 791.
- Prasad, R.: 1967, *Phys. Fluid B* **10**, 2612.
- Roux, A.: 1974, in McCormac, B. M. (ed.), *Magnetospheric Physics*, D. Reidel, Hingham, Mass, pp. 297–.
- Sazhin, S. S.: 1993, *Whistler Mode Waves in Hot Plasma*, Cambridge University Press, New York.
- Stix, T. H.: 1962, *The Theory of Plasma Waves*, McGraw-Hill, New York.
- Summers, D. and Thorne, R. M.: 1991, *Phys. Fluids B* **8**, 1835.
- Summers, D., Xue, S., and Thorne, R. M.: 1994, *Phys. Plasma* **1**, 2012.
- Tanaka, Y., Lagoutte, D., Hayakawa, M., Lefeuvre, F., and Tajima, S.: 1987, *J. Geophys. Res.* **92**, 7551–7559.
- Tripathi, A. K. and Misra, K. D.: 2001, *Indian J. Radio Space Phys.* **30**, 279.
- Tripathi, A. K. and Misra, K. D.: 2002, *Earth, Moon, Planets* **88**, 131.
- Vasyliunas, V. M.: 1968, *J. Geophys. Res.* **73**, 2839.

- Vomvoridis, J. L., Crystal, T. L., and Denavit, J.: 1982, *J. Geophys. Res.* **87**, 1473–1489.
- Xue, S., Thorne, R. M., and Summers, D.: 1996, *J. Geophys. Res.* **101**, 15457.
- Zhang, Y., Matsumoto, H., and Omura, Y.: 1993, *J. Geophys. Res.* **98**, 21353.